U

SECURIT

AD-A234 964

ITATION PAGE

Form Approved
OMB No. 0704-0188

1a REPC
Unclassified

1b. RESTRICTIVE MARKINGS

2a. SECURITY CLASSIFICATION AUTHORITY

3. DISTRIBUTION/AVAILABILITY OF REPORT
Approved for Public Release; distribution unlimited.

2b. DECLASSIFICATION/DOWNGRADING SCHEDULE

4. PERFORMING ORGANIZATION REPORT NUMBER(S)
ONR 1989

5. MONITORING ORGANIZATION REPORT NUMBER(S)

6a. NAME OF PERFORMING ORGANIZATION
National Institute of Standards & Technology

6b. OFFICE SYMBOL (If applicable)

7a. NAME OF MONITORING ORGANIZATION
Office of Naval Research

6c. ADDRESS (City, State, and ZIP Code)
Ultrasonic Standards Group
Sound A147
Gaithersburg, MD 20899

7b. ADDRESS (City, State, and ZIP Code)
Physics Division, Code 1112
Arlington, VA 22217-5000

8a. NAME OF FUNDING/SPONSORING ORGANIZATION

8b. OFFICE SYMBOL (If applicable)

9. PROCUREMENT INSTRUMENT IDENTIFICATION NUMBER
N00014-89-F-0002

8c. ADDRESS (City, State, and ZIP Code)

10. SOURCE OF FUNDING NUMBERS

PROGRAM ELEMENT NO.	PROJECT NO.	TASK NO.	WORK UNIT ACCESSION NO.
61153N	4126303		

11. TITLE (Include Security Classification)
Ultrasonic Measurements Research: Progress in 1989

12. PERSONAL AUTHOR(S)
Breckenridge, F.R., Proctor, T.M., Hsu, N.N., Fick, S.E., Eitzen, D.G.

13a. TYPE OF REPORT	13b. TIME COVERED	14. DATE OF REPORT (Year, Month, Day)	15. PAGE COUNT
Annual Summary	FROM 881001 TO 890931	890728	11

16. SUPPLEMENTARY NOTATION
This is a summary. References give more complete reporting.

17. COSATI CODES		
FIELD	GROUP	SUB-GROUP
20	01	
17	01	

18. SUBJECT TERMS (Continue on reverse if necessary and identify by block number)
Ultrasonics, physical acoustics, acoustic emission, transducers, calibration

19. ABSTRACT (Continue on reverse if necessary and identify by block number)
A prototype transfer calibration system was constructed and demonstrated to be workable. Results from elastic impact experiments were found to be in good agreement with theory. Exact results of transient wave propagation of a layered half space with different interface conditions are reported.

20 DISTRIBUTION/AVAILABILITY OF ABSTRACT
☒ UNCLASSIFIED/UNLIMITED ☐ SAME AS RPT ☐ DTIC USERS

21. ABSTRACT SECURITY CLASSIFICATION
Unclassified

22a NAME OF RESPONSIBLE INDIVIDUAL	22b TELEPHONE (Include Area Code)	22c OFFICE SYMBOL
L. E. Hargrove, ONR Physics Division	202-969-4221	ONR Code 1112

DD Form 1473, JUN 86 Previous editions are obsolete 646 SECURITY CLASSIFICATION OF THIS PAGE

UNCLASSIFIED

Ultrasonic Measurements Research: Progress in 1989

F.R. Breckenridge, T.M. Proctor, N.N. Hsu,
S.E. Fick and D.G. Eitzen

Ultrasonic Standards Group
National Institute of Standards and Technology

ABSTRACT

A prototype transfer calibration system was constructed and demonstrated to be workable. Results from elastic impact experiments were found to be in good agreement with theory. Formulas have been derived for the calculation of Green's functions for multi-layered media, and computer code has been written for calculation of Green's functions for single layered media.

TRANSFER CALIBRATION OF ACOUSTIC EMISSION TRANSDUCERS

The design of a practical and reasonably accurate prototype transfer calibration system for acoustic emission (AE) transducers has evolved in the past year. This year's work involved the use of a 20 cm thick block which replaced the 3.3 cm thick plate that was found to be unsuitable in last year's work.

The calibration scheme used as a test of the suitability of the transfer block is very similar to that of the primary calibration. The test scheme uses a capillary-break source located near the center of one of the large faces of the block and has the transducer under test and the reference transducer each located 10 cm from the source, but in opposite directions, as shown in Fig 1. The capillary break produces, on the surface of the block, a pulse which, because of geometric symmetry, excites both transducers equally. Transient waveforms from both transducers are captured, analyzed for frequency content, and compared. A correction based on the primary calibration of the reference transducer is applied in calculating the final calibration data for the transducer under test.

This transducer calibration scheme had been tested by early FY89 using a steel plate 90 cm square by 3.3 cm thick. The size and shape had been chosen to obtain a large area, allowing a long working time, and an overall weight affording some portability compared to that of the primary reference block. Experimental results later showed that in trading off area, thickness, and overall bulk, the thickness of the plate was reduced excessively. Trial calibrations utilizing both capillary-break and tone-burst schemes were performed on this plate, and the calibration results showed no agreement with the primary calibration results for the same test transducers. The discrepancies can be attributed to excessive variations in the surface displacement of the plate underneath the transducer being calibrated. Such variations would (in hindsight) be expected to be significant when the diameter of the transducer is comparable to the thickness of the plate. We intend to pursue

investigation of the problem of disparate motion within the aperture of a circular transducer on a plate by a theoretical analysis which uses an integration technique applied to the Green's function for the elastic plate.

The new transfer calibration system utilizes a steel transfer block 40 cm square and 20 cm thick. This block, mounted on casters, is reasonably portable. In the interests of good ultrasonic coupling, it is necessary that at least one of the block's 40 cm square faces have a high quality finish. Either surface grinding or Blanchard grinding produces a result that is good enough for the purpose. Since Blanchard grinding was offered by the vendor, that process was used to finish both square faces of our block. The block cost only $800 for the material and its surface preparation.

The block for the transfer calibration system is approximately half the size, in linear dimensions, of the primary calibration block. Therefore, the working time between arrival of the calibration signal and the arrival of its first reflection from the walls of the block is only about half of that for the primary block. For transducers that have a long ringing time when shock excited, the accuracy of the small-block calibration is less. This effect might be expected to be prominent mainly at the low end (100 kHz) of the frequency range.

To evaluate the transfer calibration method, six transducers were calibrated using the primary calibration system and also using the proposed transfer calibration system. Three models of transducer were represented among the six. The best results were obtained for an NBS conical transducer, for which agreement was within ±1 dB for almost all points over the calibration frequency range of 100 kHz to 1 MHz (Fig 2). One model of commercial ultrasonic/AE transducer produced results that were in agreement within ±1 dB for almost all points except for frequencies above 750 kHz, where the disagreement became as large as 11 dB (Fig 3). For another model of commercial AE transducer the agreement was within ±2 dB almost everywhere, which is approximately as well as the primary calibration can be repeated for this model (Fig 4).

ELASTIC IMPACT EXPERIMENTS

The study of the impact of elastic spheres on an elastic plate has triple significance: Firstly, the impact source has possible application in other AE experiments and in non destructive testing, secondly, the development of the technique whereby the signature of a source event may be characterized is important, and thirdly, the experimental validation of the theoretical Green's function and deconvolution techniques used in this experiment is essential to all AE studies.

The scheme of the elastic impact experiment is shown in Fig 5.
In the experiment, steel balls of various sizes were dropped onto a glass plate from a height of 3 cm. A calibrated NBS conical transducer, located on the plate opposite the point of impact, was used to record the displacement of the plate at the transducer location. Deconvolution by

the plate Green's function and the transducer response yielded the force versus time waveform of the source.

Calibration of the conical transducer was performed on the same glass plate that was used in the experiment, because transducer calibration is dependent on the elastic properties of the driving medium. To calibrate the transducer, glass capillaries were broken at a point on one flat surface of the plate, with the transducer located on the other surface and opposite the source. Waveforms from eight calibration events were captured, and for each, the force of the capillary break was measured. It was assumed that the glass-break event applied a Heaviside force to a point on the surface of the glass plate. The captured output waveform from the NBS conical transducer should, therefore, be $F_0 \times H(t) * G(t) * T(t)$, where F_0 is the magnitude of the Heaviside force, H(t) is the Heaviside function, G(t) is the Green's function for the plate, and T(t) is the impulse response of the transducer. Since F_0 is known from the force measurement and G(t) is known from theory, the impulse response of the transducer can be extracted from the captured waveform data by division, differentiation, and convolution operations. The impulse response of the transducer so obtained is inverted with respect to the convolution operation for its subsequent use in the ball-drop part of the experiment. Balls were dropped onto the same spot of the glass plate where the capillary breaks took place, and waveforms from the NBS conical transducer were captured as before. Now, the captured waveform should be $B(t) * G(t) * T(t)$, where B(t) is the force waveform produced by the ball's impact on the plate. B(t) is extracted from the captured data by convolution operations using the known G(t) and T(t). The computational procedures are charted in Fig 6.

We devised a numerical integration procedure based on Hertz's theory to calculate the theoretical time waveform for an elastic sphere colliding with an elastic plate. The theoretical time waveform so obtained compares very favorably with the results of the dropping ball experiments. Fig 7 shows the theoretical time waveform and the experimental waveform obtained from the single dropping of a 9.52 mm ball. The theoretical data for the curve of Fig 7 has been multiplied by 0.9713 for reasons discussed below.

In the elastic collision experiment, there were ten balls, each of a different size. The number of dropping events for each size was between seven and ten. For each ball, the average peak force excursion relative to the theoretically predicted force excursion is shown in Table I. The relative peak force excursion averaged for all events is 0.9505; i.e., the impulses obtained in the experiments were small by approximately 5%.

The fact that the experimentally obtained impulses were small is not surprising. It is expected that there would be losses owing to sound radiated into the plate and into the air, and possibly other losses owing to air resistance and imperfect elasticity, which are not accounted for in the theory. We calculate that for an impulse that is 0.95 times the theoretical value, there would correspond a coefficient of restitution (ratio of emerging to impinging speed of the ball) of 0.90. Typically

coefficients of restitution do not exceed 95% in such experiments.

The favorable results obtained in the elastic collision experiment validate the use of the technique as a tool to obtain the signature of any impulsive type of source applied to the surface of a plate.

TRANSIENT GREEN'S TENSOR FOR LAYERED MEDIA

Pulsed ultrasonic testing techniques have been proposed for a greater role in the evaluation and quality control of composite materials. The understanding of the interaction between ultrasonic waves and interfaces in a layered material constitutes an important part of the development of the technology.

The solution of the problem of calculating the Green's tensor for an isotropic layer overlay on an isotropic half space was reported last year. During the current year we have successfully completed the design of algorithms and FORTRAN code to facilitate calculating solutions to this problem assuming three different bonding conditions between the layer and the substrate. In Fig 8 are sample results of the computation. These curves represent the computed normal displacement as a function of time due to a point contact source transducer whose force waveform is a damped sinusoid. The bonding conditions for the three cases are: (A) no bond--the boundary stresses are zero, (B) welded bond--both stress and displacement are continuous across the boundary, and (C) liquid bond--normal stress and normal displacement are continuous at the boundary and tangential stresses are zero. A head wave is apparent as the centrally located pulse in trace (B), but is absent in trace (A) and highly suppressed in trace (C). It is expected that in experimental waveforms, the presence or absence of the headwave can be used to deduce the condition of the bond.

During the current year, we have successfully completed a derivation, based on J. Willis's method, of the formulas for a multi-layer structure.

TABLE I

Summary of Ball-Drop Data

Ball Diameter	Peak Force (Experiment/Theory)	Number of Events
9.520 mm	0.9713	7
7.935	0.9587	9
7.134	0.9614	9
6.347	0.9469	8
5.555	0.9557	9
4.760	0.9535	9
3.967	0.9552	9
3.170	0.9254	9
2.377	0.9531	10
1.582	0.9280	9
Average	0.9505	Total 88

FIGURE CAPTIONS

Fig 1. Block diagram of the capillary-break scheme for transfer calibration of AE transducers.

Fig 2. Comparison of a primary and a transfer (secondary) calibration performed on an NIST standard reference conical transducer (SRM 1856).

Fig 3. Comparison of primary and transfer (secondary) calibrations performed on a commercial ultrasonic/AE transducer. The solid curve represents the average of four primary calibrations; the dashed curve represents a single transfer calibration.

Fig 4. Comparison of primary and transfer (secondary) calibrations performed on an AE transducer. The solid curve represents the average of four primary calibrations; the dashed curve represents a single transfer calibration. Primary calibration for this transducer shows more variability than for most others.

Fig 5. Scheme of the ball-drop experiment. The dimensions of the glass plate are: diameter = 42 cm, thickness = 8.9 cm.

Fig 6. Calculation diagram for the elastic impact experiment. The "*" indicates convolution and the "-1" superscript indicates the convolutional inverse. F_0 is the measured value of the force of the capillary break. The other letters all indicate functions of time: B is the ball-drop force, H is the Heaviside function, G is the Green's function for the plate, and T is the transducer impulse response.

Fig 7. Elastic sphere collision experiment: The lower curve is the force signature of an elastic ball colliding with an elastic plate as calculated from Hertz's theory. The upper curve is the output from an NBS conical transducer after deconvolution by the Green's function for the plate and the impulse response of the transducer. The values for the theoretical curve have been multiplied by 0.9713, and the experimental curve has been elevated by 0.2.

Fig 8. Theoretically computed Green's functions, G_{33}, for a plexiglass layer on a semi-infinite glass substrate when both source and detector are located on the top surface of the layer and the distance between them is three times the thickness of the layer. The input force is an exponentially decaying sine function, shown as an inset in the figure. The longitudinal and shear wave speeds are, respectively, for the plexiglass: 2730, 1430, and for the glass: 5830, 3490, and the densities are for the plexiglass: 1180, and for the glass: 2500 in mks units. The three curves correspond to boundary conditions of the interface: A, traction free; B, welded; C, liquid coupled.

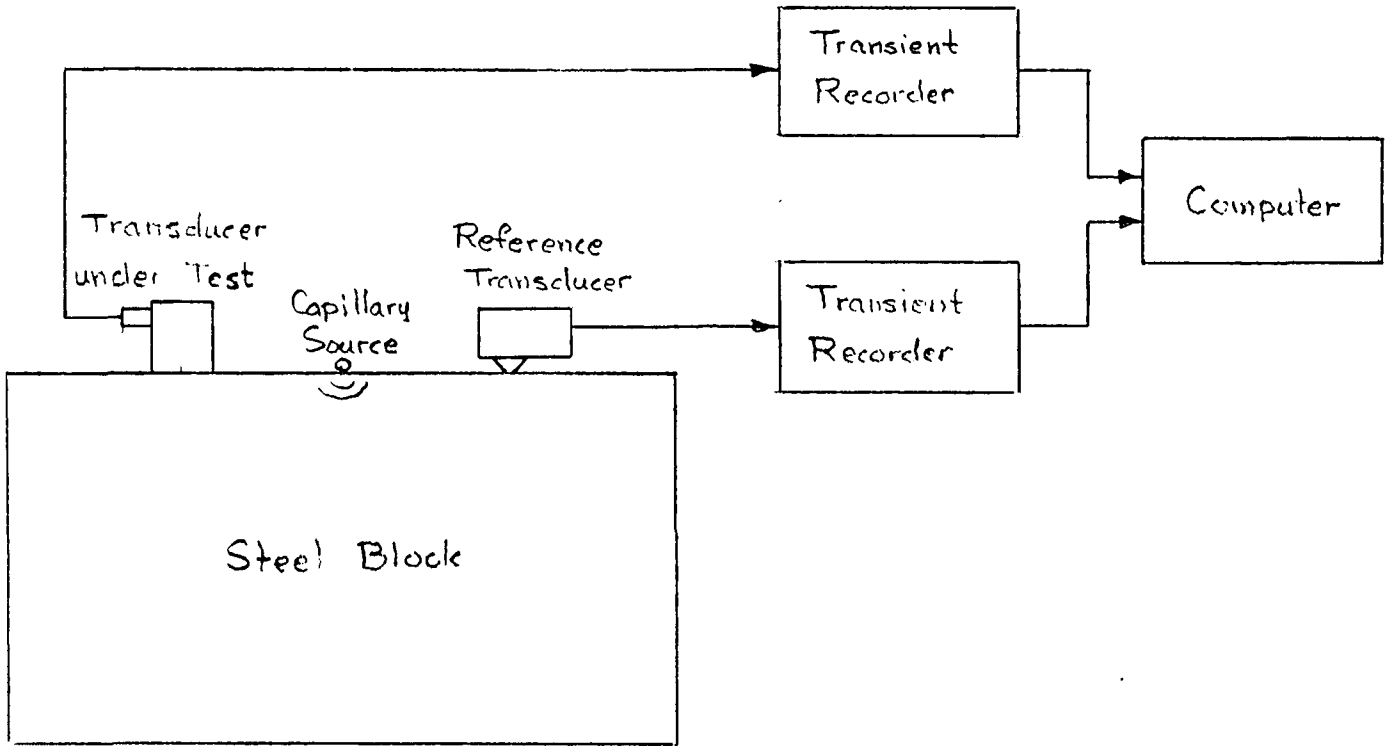
Transient
Recorder
Computer
Transducer
under Test
Capillary
Source
Reference
Transducer
Transient
Recorder
Steel Block

Fig 1

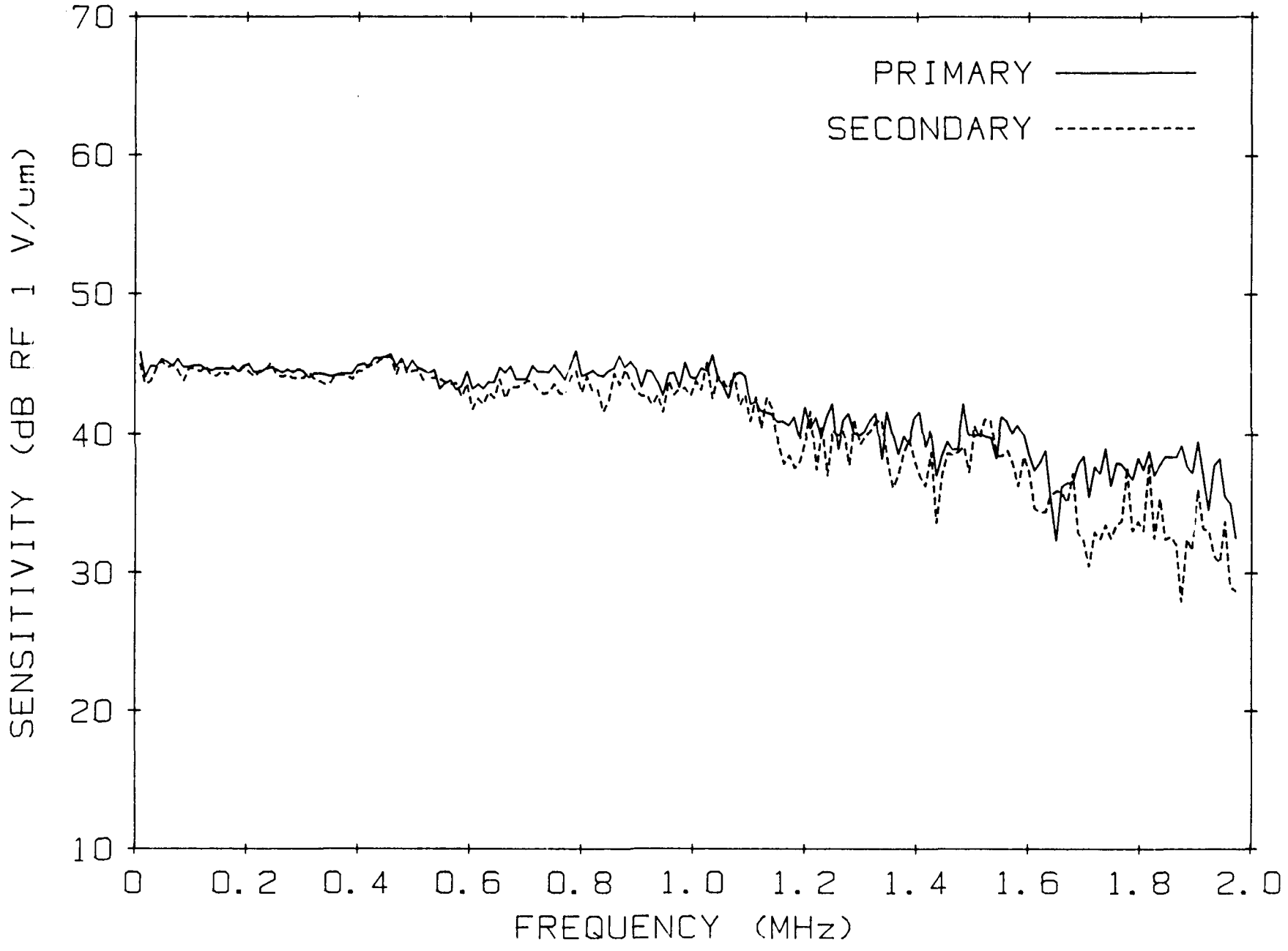
70
60
50
40
30
20
10
SENSITIVITY (dB RF 1 V/um)
PRIMARY
SECONDARY
0
0.2
0.4
0.6
0.8
1.0
1.2
1.4
1.6
1.8
2.0
FREQUENCY (MHz)

Fig 2

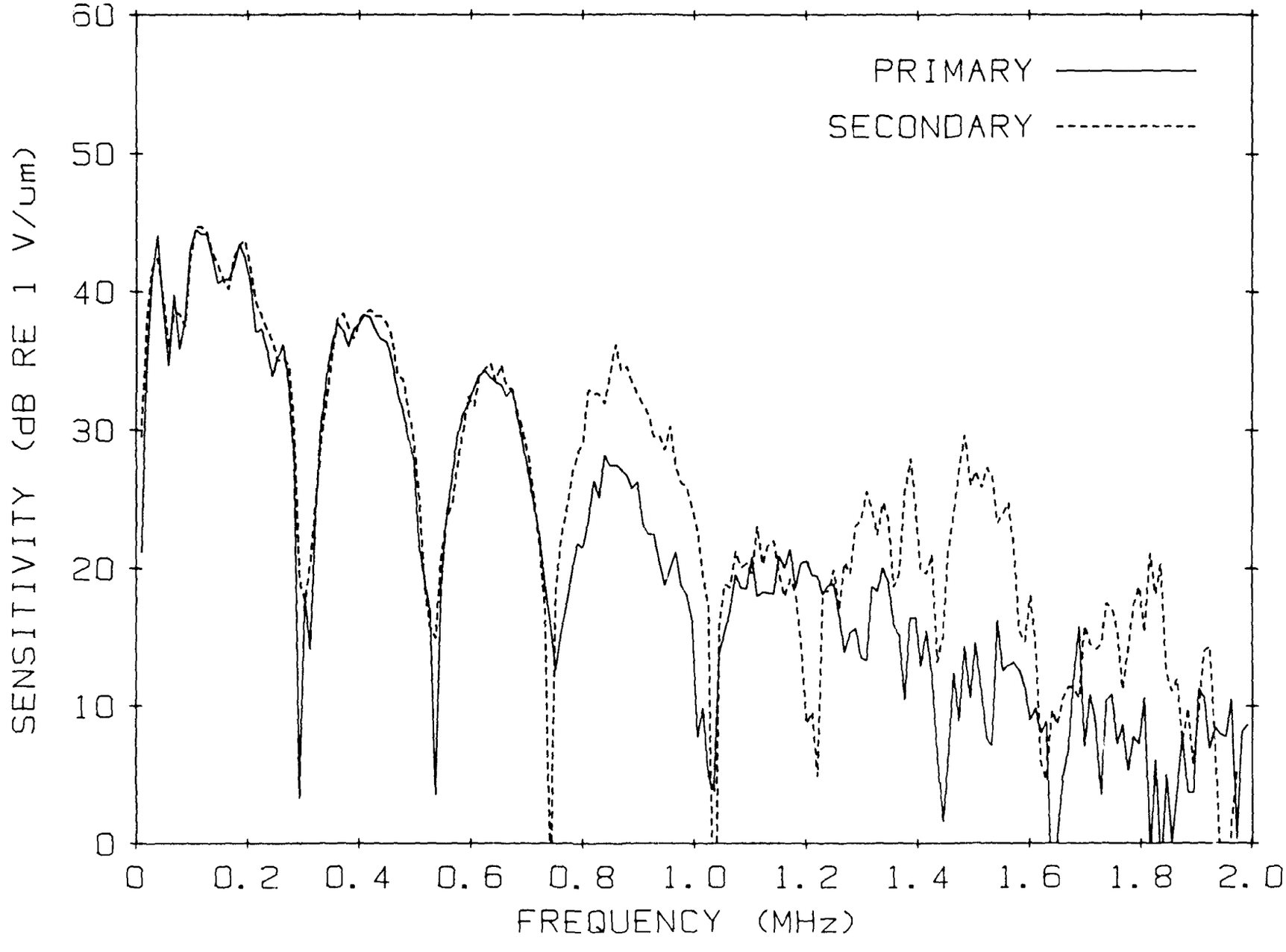
PRIMARY
SECONDARY
SENSITIVITY (dB RE 1 V/um)
60
50
40
30
20
10
0
0
0.2
0.4
0.6
0.8
1.0
1.2
1.4
1.6
1.8
2.0
FREQUENCY (MHz)

Fig 3

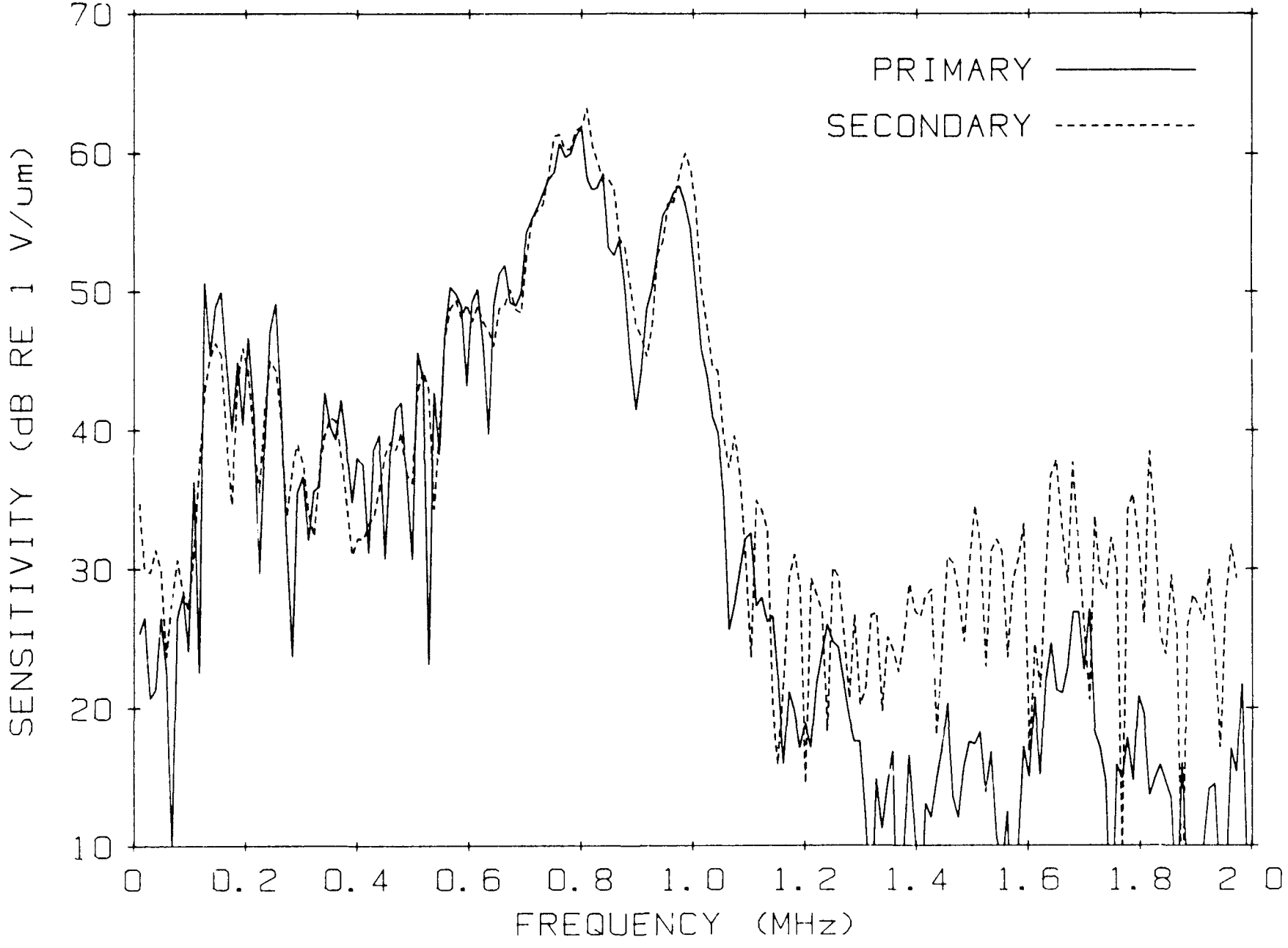
PRIMARY
SECONDARY
SENSITIVITY (dB RE 1 V/um)
70
60
50
40
30
20
10
0
0.2
0.4
0.6
0.8
1.0
1.2
1.4
1.6
1.8
2.0
FREQUENCY (MHz)

Fig 4

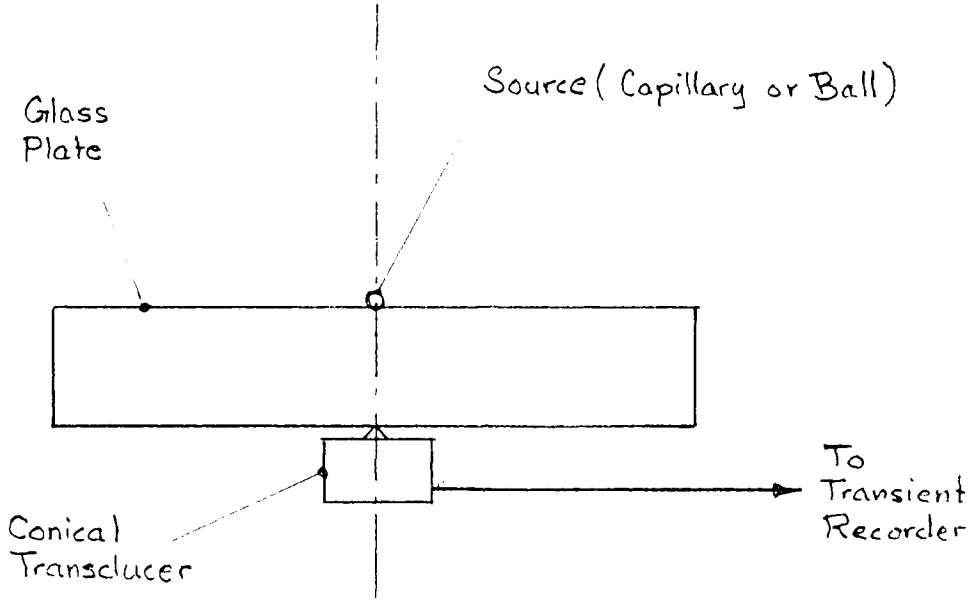
Source (Capillary or Ball)
Glass
Plate
To
Transient
Recorder
Conical
Transducer

Fig 5

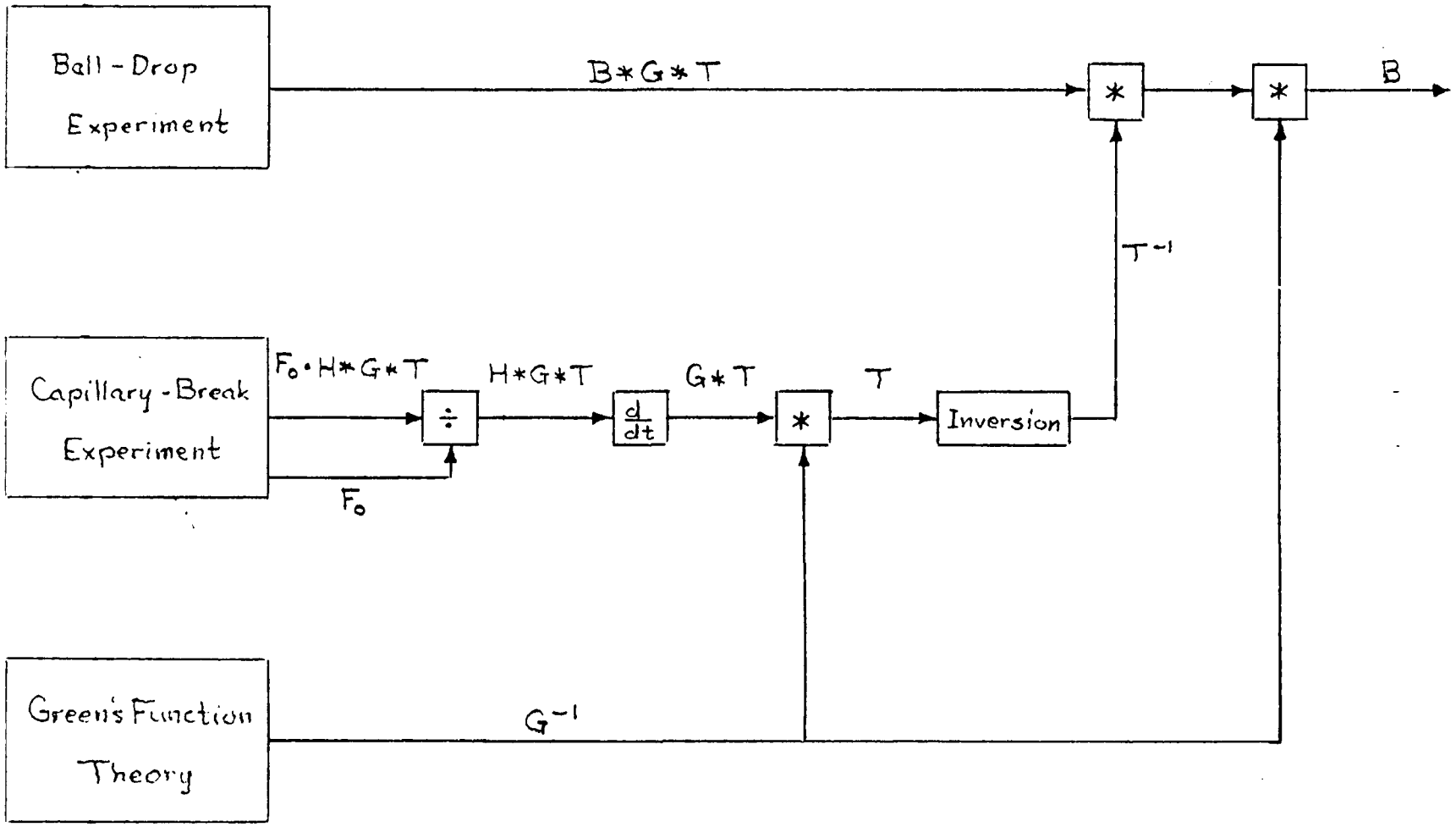
Ball - Drop Experiment
B*G*T
*
*
B
T⁻¹
Capillary - Break Experiment
F₀·H*G*T
÷
H*G*T
d/dt
G*T
*
T
Inversion
F₀
Green's Function Theory
G⁻¹

Fig 6

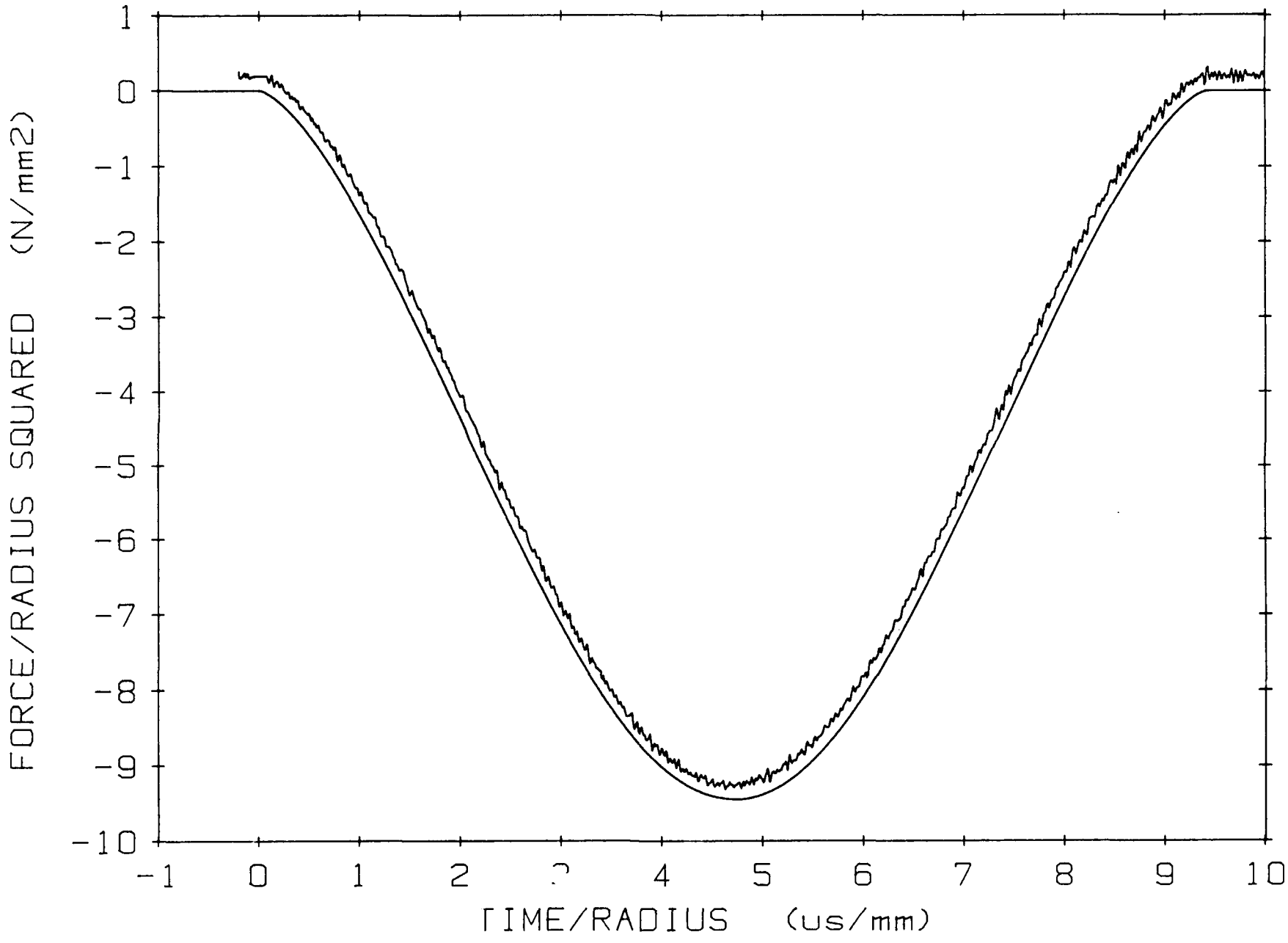
FORCE/RADIUS SQUARED (N/mm2)
1
0
-1
-2
-3
-4
-5
-6
-7
-8
-9
-10
-1
0
1
2
4
5
6
7
8
9
10
TIME/RADIUS (us/mm)

Fig 7

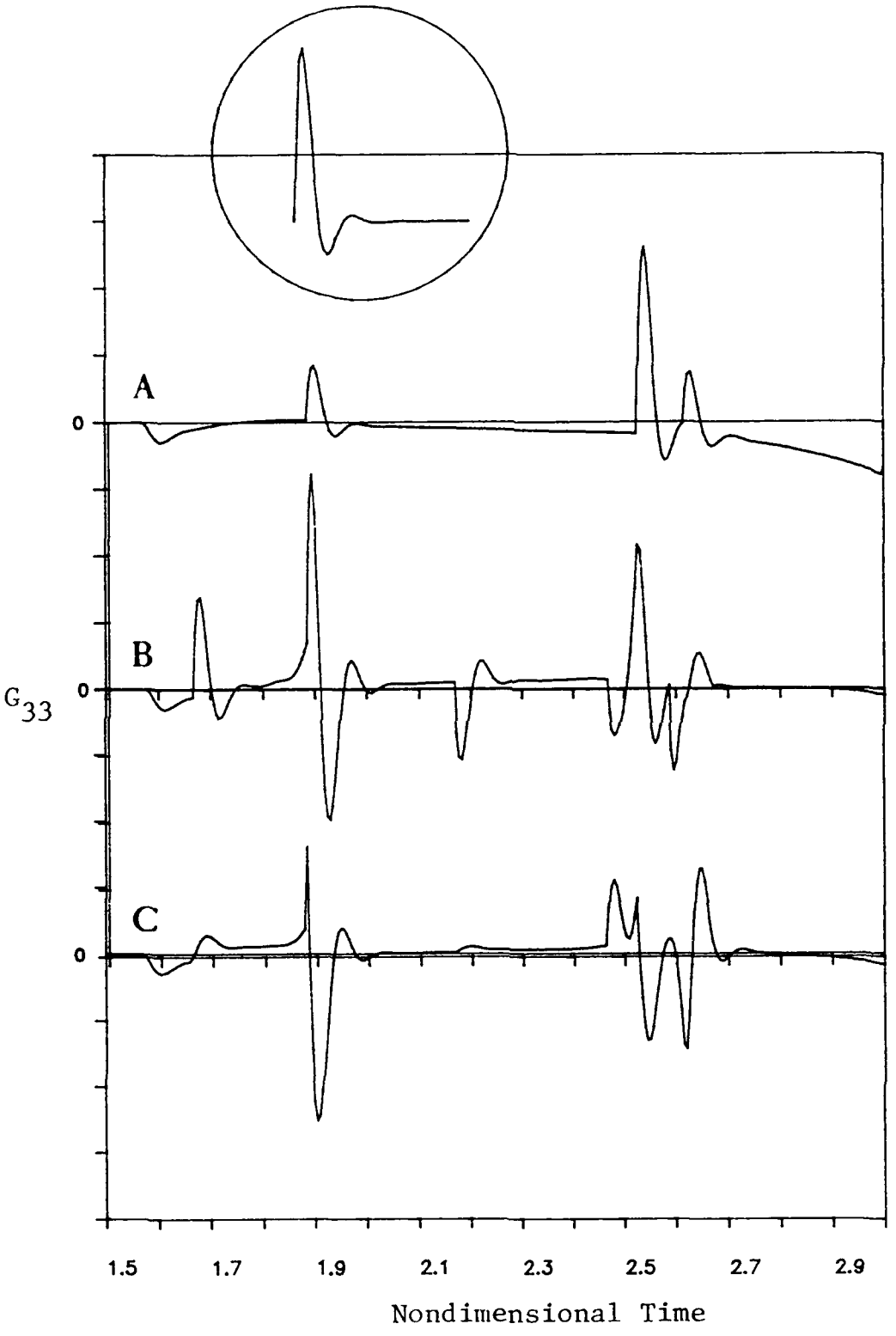

Fig 8